The memoirs of Faculty of Engineering
Fukuyama University
The 26 th issue, Sep., 2002

Investigation of Flowfield around Hypersonic Space Plane

Hiroaki NAKAMURA*, Shinji SEZAKI*, Keiji MANABE**, and Masatomi NISHIO**

ABSTRACT

The flowfield analysis around a model of space plane traveling at Mach 10 has been carried out utilizing the Electric Discharge Method [1-3] and the Finite Element Method (FEM) scheme [4], [5] The Electric Discharge Method can be visualized almost all important hypersonic flowfield phenomena, such as three-dimensional shock shapes, streamlines near wall surface, distant streamlines from wall surface, and boundary layers etc. In this study, the experiments and the numerical simulations were carried out under the conditions the angles of attack were 0 and 10 deg. Furthermore, the experimental results were compared with the numerical ones. In these comparisons, it was found that they were relatively in good agreement.

Keywords : Space Plane, Hypersonic Flow, Electric Discharge Method, and Finite Element Method

1. Introduction

As space activities increase and transportation between the earth and space has become more frequent, a totally new transportation system called a Space Plane (SSTO : Single-Stage-To-Orbit) is now under development. In this system, it is expected to cut down transportation costs drastically. Therefore, it is important to understand the hypersonic flowfeild around the hypersonic vehicle to develop it.

However, there are very few experimental results. The author and others have developed a method for visualizing various kinds of flowfield phenomena, such as three-dimensional shock shapes, streamlines near wall surface, distant streamlines from wall surface, and boundary layers etc. It is called the Electric Discharge Method.

On the other hand, the Computational Fluid Dynamics (CFD) technology is useful method for analysis of the flowfield because of the computer development. Especially, the flowfield around the hypersonic vehicle is mainly calculated by the Finite Difference Method (FDM). In this study, a calculation method for hypersonic flowfield is developed based on the FEM.

In flowfield around Space Plane traveling at Mach 10, the visualized results by the Electric Discharge Method and the calculated ones by the FEM are shown.

2. Experimental Method

The experiments were carried out utilizing the

* Graduate student, Department of Mechanical Engineering

** Department of Mechanical Engineering

hypersonic gun tunnel shown in Fig.1. The main characteristics of the tunnel are as follows: the Mach number is 10, the duration is 10ms, the freestream density is 4.5×10^{-3}kg/m^3, and the test gas is air. The dimensions of model used in the experiments are shown in Fig.2.

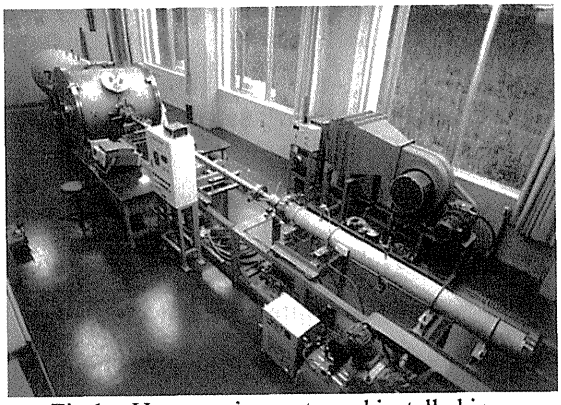

Fig.1 Hypersonic gun tunnel installed in Fukuyama University. (M=10)

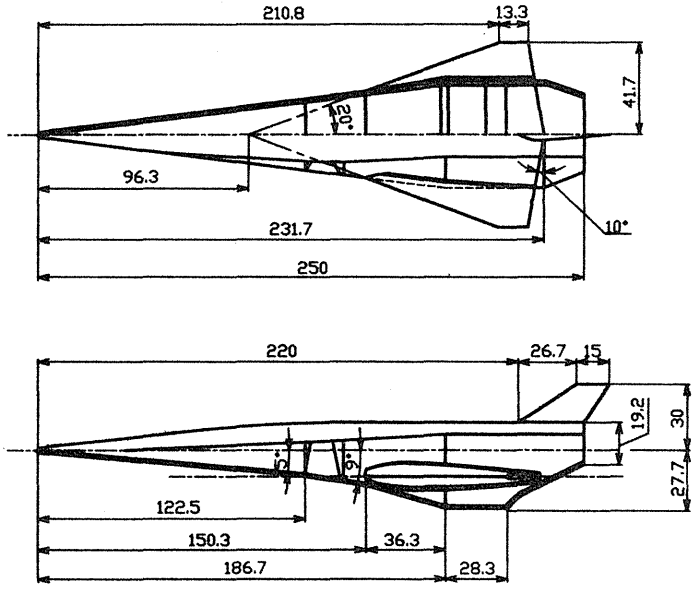

Fig.2 Model dimensions of Space Plane.

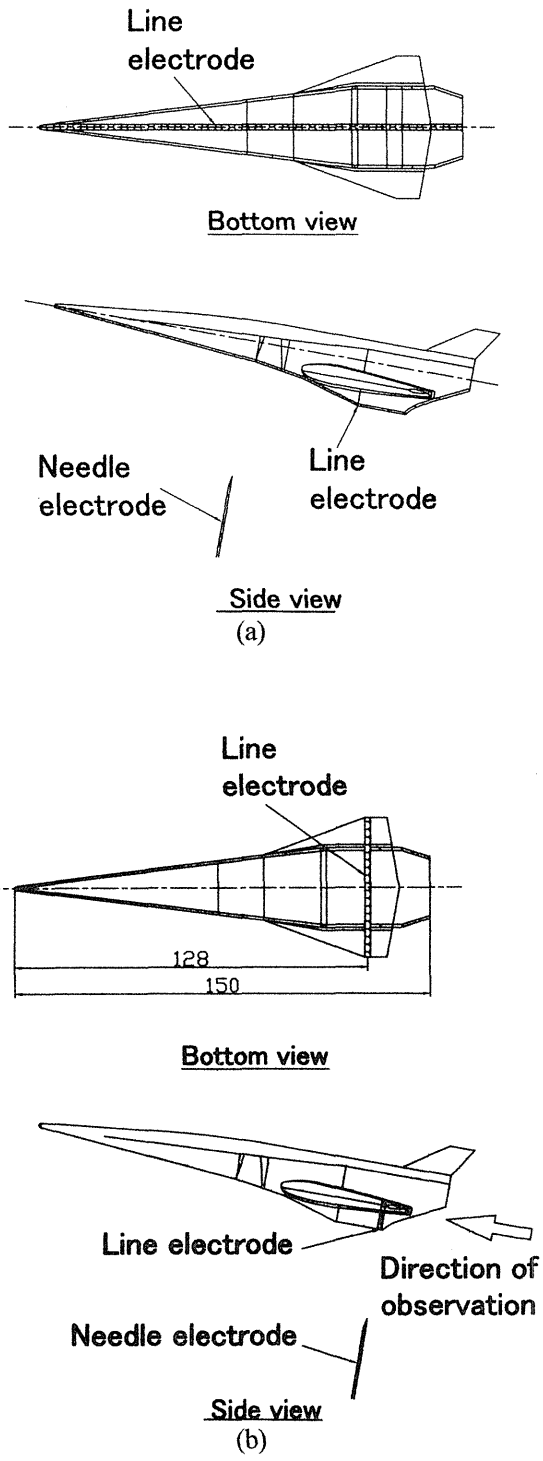

Fig.3 Arrangement of a pair of electrodes.

Subsequently, the principle of visualizing three-dimensional shock shapes around a model of Space Plane is shown. The arrangement of a model and a pair of electrodes are shown in Fig.3. In this case, the cathode needle electrode is set in the freestream. The anode line electrode is bonded to the surface of model. The line electrode should be very thin so as not to disturb the flow. The line electrode is 0.1mm thick and 2mm wide. The principle of visualizing shock wave is based on the following idea. When an electric discharge is generated across the shock wave, we can see a dark position where the shock wave exists in the electric discharge path. Because, at the shock wave location, the level of electron excitation of gas molecules become very low and the radiation intensity from the position becomes very weak. Consequently, the shock wave can be visualized by taking

a photograph of the electric discharge path. As an example, the visualized result of the shock wave over a wedge model is shown in Fig.5.

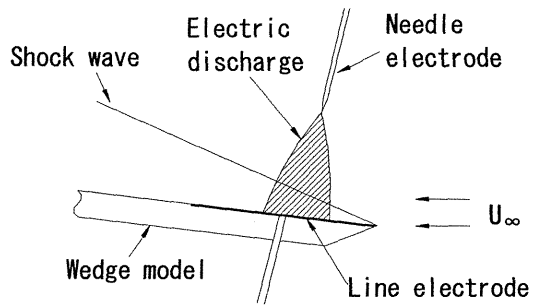

Fig.4 Principle of visualizing shock wave.

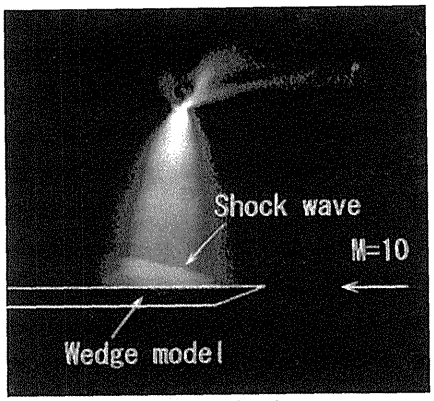

Fig.5 Visualization of the shock wave over a wedge model.

3. Computational Method

In the numerical calculations, the compressible Navier-Stokes equations were used. The compressible Navier-Stokes equations in conservation form is as follows:

$$\frac{\partial \mathbf{U}}{\partial t}+\left(\frac{\partial \mathbf{F}_1}{\partial x}+\frac{\partial \mathbf{F}_2}{\partial y}+\frac{\partial \mathbf{F}_3}{\partial z}\right)-\left(\frac{\partial \mathbf{G}_1}{\partial x}+\frac{\partial \mathbf{G}_2}{\partial y}+\frac{\partial \mathbf{G}_3}{\partial z}\right)=0 \quad (1)$$

where each vector is expressed as follows:

$$\begin{cases} \mathbf{U}=\{\rho \;\; \rho u_x \;\; \rho u_y \;\; \rho u_z \;\; \rho e\}^T \\ \mathbf{F}_1=\mathbf{U}u_x \\ \mathbf{F}_2=\mathbf{U}u_y \\ \mathbf{F}_3=\mathbf{U}u_z \\ \mathbf{G}_1=\{0 \;\; T_{xx} \;\; T_{xy} \;\; T_{xz} \;\; u_xT_{xx}+u_yT_{xy}+u_zT_{xz}-q_x\}^T \\ \mathbf{G}_2=\{0 \;\; T_{xy} \;\; T_{yy} \;\; T_{yz} \;\; u_xT_{xy}+u_yT_{yy}+u_zT_{yz}-q_y\}^T \\ \mathbf{G}_3=\{0 \;\; T_{xz} \;\; T_{yz} \;\; T_{zz} \;\; u_xT_{xz}+u_yT_{yz}+u_zT_{zz}-q_z\}^T \end{cases} \quad (2)$$

The notations in Eq.(2) has the following meaning:
ρ=density [kg/m^3], u_x, u_y, u_z=velocity components in x, y, and z directions [m/s], e= total energy [J], T_{xx}, T_{xy}, T_{xz}, T_{yz}, T_{zz}=stress [Pa], and q_x, q_y, q_z=heat flex in x, y, and z directions [J/kg].

The stress is expressed as follows:

$$T_{ij}=\tau_{ij}-p\delta_{ij} \quad (3)$$

In Eq.(3), τ_{ij}=viscous stress [Pa], p=pressure [Pa], δ_{ij}=Kronecker delta.
Furthermore, the pressure is given by:

$$p=(\kappa-1)\rho\left(e-\frac{1}{2}u_k u_k\right) \quad (4)$$

Next, as boundary conditions, they are based on the relations.

$$\mathbf{U}=\bar{\mathbf{U}}(\text{on}S_U), \quad \mathbf{G}_1n_x+\mathbf{G}_2n_y+\mathbf{G}_3n_z=\bar{\mathbf{P}}(\text{on}S_P) \quad (5)$$

where u_x, u_y, u_z=unit normal vector in x, y, and z directions.

The formulation for FEM is carried out based on the weighted residual method (Galerkin Method). The weighted function w which takes value 0 on the surface S_U was considered. We multiply w on Eq.(1) and integrate it over the region V. Equation (1) becomes as follows:

$$\begin{aligned}\int_V w\frac{\partial \mathbf{U}}{\partial t}dV=&-\int_V w\left(\frac{\partial \mathbf{F}_1}{\partial x}+\frac{\partial \mathbf{F}_2}{\partial y}+\frac{\partial \mathbf{F}_3}{\partial z}\right)dV \\ &-\int_V\left(\frac{\partial w}{\partial x}\mathbf{G}_1+\frac{\partial w}{\partial y}\mathbf{G}_2+\frac{\partial w}{\partial z}\mathbf{G}_3\right)dV \\ &+\int_{Sp}w\bar{P}dS \end{aligned} \quad (6)$$

As shown in Eq.(6), the pressure p in the Navier-Stokes equations are expressed by the non-differential form to improve the accuracy in calculation. This method is usually used for simulation the deformation of solid such as elastic materials and elastic-plastic materials.

In order to introduce the upwind effect for the analysis, the SUPG (Streamline Upwind Petrov-Galerkin) method is used. Furthermore, the explicit scheme is used for

time integration by making left hand of Eq.(6) diagonal matrix. By this procedure, it does not need to solve the simultaneous equations. Therefore, the calculation time and computer memory can be saved.

The validity of this application was examined by comparing the computational result with the one of Schlieren. In this comparison, the wedge model was used. The results are shown in Fig.6. In this picture, the centerline marks the boundary between the computational result and the experimental result. That is, the upper part of the figure is the computational result and the lower part of the picture is the experimental result. From this comparison, it was found that they were in

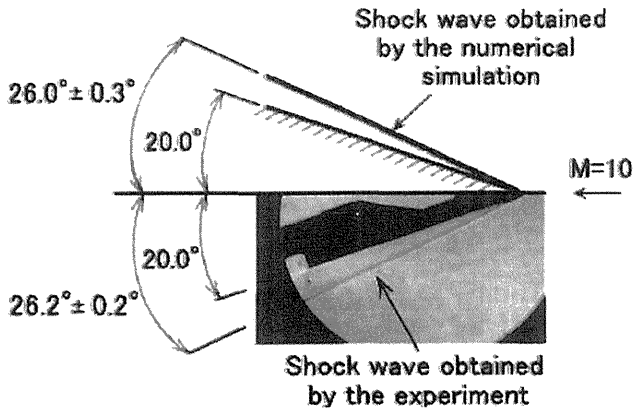

Fig.6 The comparisons between the computational result and the experimental result.

4. Experimental Results

First, the lateral shock shapes of the model in the hypersonic flow were visualized. As a method of visualizes, Figure 3 (a) was used. In Fig.3 (a), the sheet-shaped electric discharge is generated between the electrodes applying a high voltage of 2 kV. The experiments were carried out under the conditions that the angle of attack of model are 0 and 10 deg. The visualized results are shown in Fig.7. In Fig.7 (a), the interaction of two shock waves generated by the nose of a model and a part of a scramjet engine were visualized. Furthermore, in Fig.7 (b), the reflected shock wave was visualized. From this result, it was found that the flowfield around a scramjet engine becomes very complicated.

Second, the cross-sectional shock shapes perpendicular to the freestream were visualized. As a method of visualizes, Figure 3 (b) was used. Figure 8 is the photograph of visualized results from the bottom side using a mirror.

Thus, the flowfield around a model, such as three-dimensional shock shapes can be visualized more easily by utilizing the Electric Discharge Method.

5. Computational Results

In this numerical simulation, the computational grid consists of $49 \times 21 \times 89$ nodal points, and non-slip boundary conditions were given for wall surface of the model. Furthermore, the flow is assumed to be a laminar. The computational grid and the freestream conditions used for calculation are shown in Fig.9 and Table 1 respectively. In Table 1, these variable values are the same ones as experimental and the Reynolds number is the value per unit length. The simulations were carried out under the condition that the angle of attack of model is 0 and 10 deg. To compare with the experimental results, the density distributions, the pressure distributions, and the temperature distributions around a model were calculated. The results are shown in Figs.10 and 11. In Fig.10, the interaction with the shock waves generated by the nose of a model and the part of a scramjet engine were calculated. Furthermore, in Fig.11, at a scramjet engine, the value for the ratio of density becomes very large. From these results, it was found that the flowfield around a scramjet engine becomes very complicated.

6. Conclusion

In this study, the flowfield around a model of Space Plane traveling at Mach 10 was investigated by the Electric Discharge Method and the FEM. The results of the survey are as follows.

(1) In the case of 0-deg angle of attack

- There are the shock-wave/shock-wave interactions around the scramjet engine.

(2) In the case of 10-deg angle of attack

- At the scramjet engine, two shock waves generate.
- The shock wave generated by a nose of a model is curved at the scramjet engine.
- Its shock wave interacts with the shock wave generated by the scramjet engine.

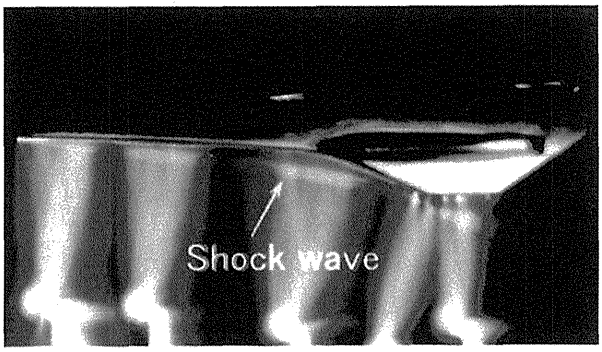

(a) 0-deg angle of attack

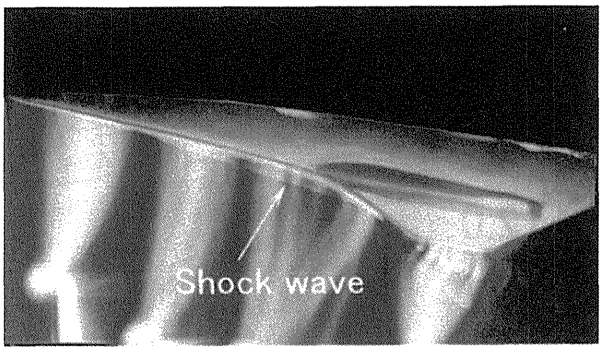

(b) 10-deg angle of attack

Fig.7 Visualized shock shapes. (from side)

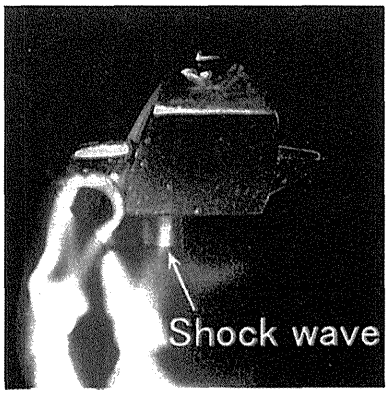

(a) 0-deg angle of attack

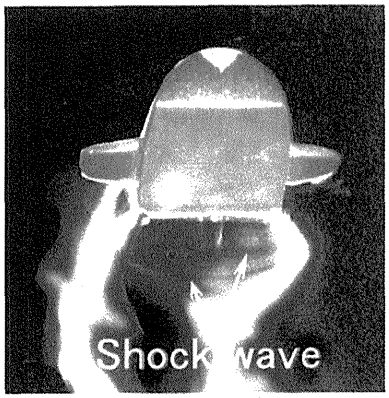

(b) 10-deg angle of attack

Fig.8 Visualized cross-sectional shock shapes.

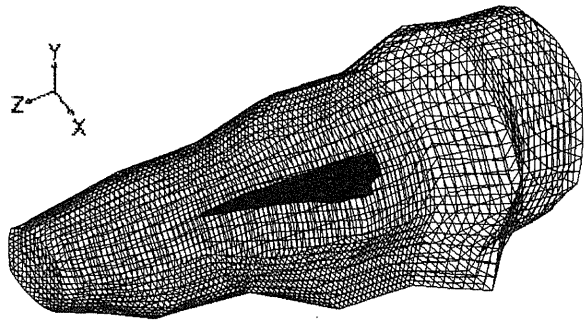

Fig.9 Computational grid around a model.

Table 1 Freestream conditions

Variable	Value	Unit
Freestream velocity	1500	m/s
Mach number	10	
Static pressure	70	Pa
Static temperature	54	K
Freestream density	4.5×10^{-3}	kg/m^3
Reynolds number	1.95×10^{6}	
Ratio of specific heat	1.4	

References

[1] Nishio, M., Hagiwara, T.:Hypersonic Flowfield Analysis of X-33 Model with the Electric Discharge Method, Journal of Spacecraft and Rockets., **36** (1999), pp.784-787.

[2] Nishio, M.:New Method for Visualizing Three Dimensional Shock Shapes around Hypersonic Vehicles Using an Electric Discharge, AIAA J., **28** (1990), pp.2085-2091.

[3] Nishio, M.:Qualitative Model for Visualizing Shock Shapes, AIAA J., **30** (1992), pp.2346-2348.

[4] Manabe, K., Nishio, M., and Sezaki, S.:Study on Flowfield Around Space Plane Traveling at Mach 10, AIAA/NAL-NASDA-ISAS 10-th International Space Plane and Hypersonic Systems and Technologies Conference, Kyoto, Japan, 2001, AIAA-2001-1796.

[5] Nakamura, H., Sezaki, S., Manabe, K., and Nishio, M.:Flowfield Around Space Plane Traveling at Mach 10 (Comparison of Visualization and Calculation), The 10th International Symposium on Flow Visualization, Kyoto, Japan, 2002, F0183.

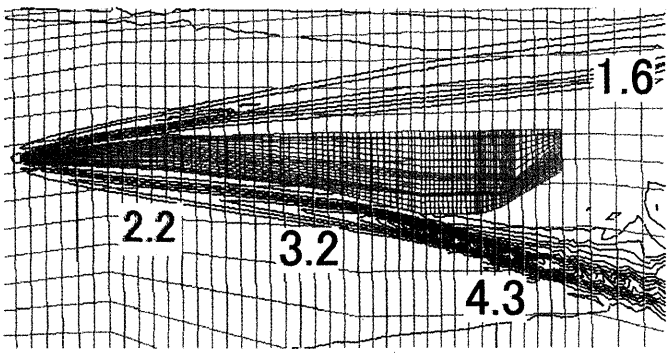

(a) Nondimensional density ρ / ρ_∞
(max ρ / ρ_∞=4.3)

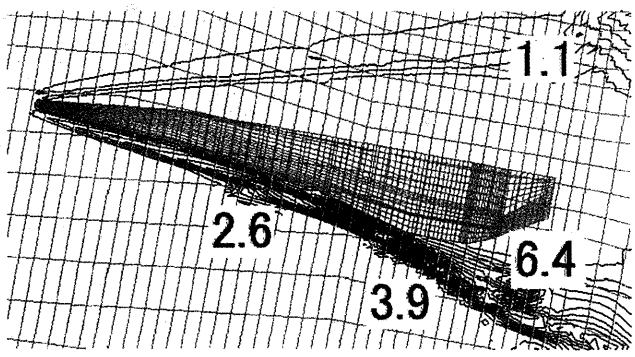

(a) Nondimensional density ρ / ρ_∞
(max ρ / ρ_∞=6.4)

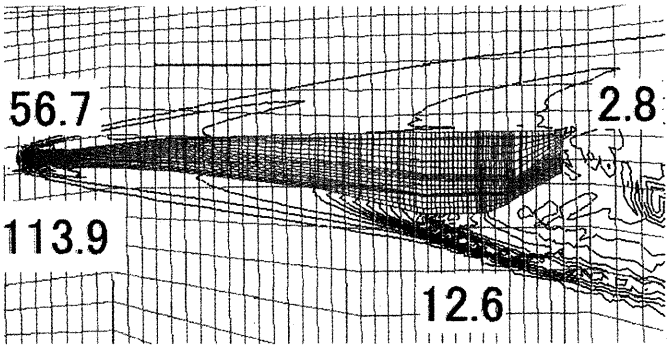

(b) Nondimensional pressure p/p_∞
(max p/p_∞=113.6)

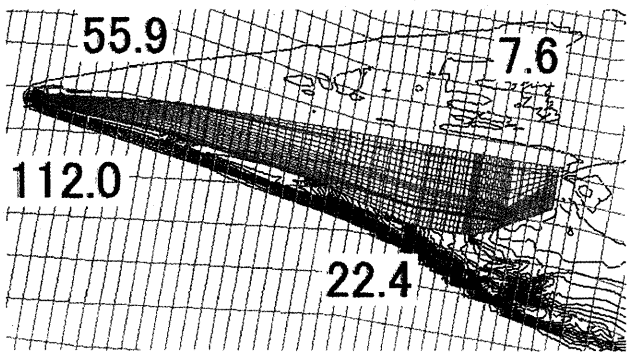

(b) Nondimensional pressure p/p_∞
(max p/p_∞=112.0)

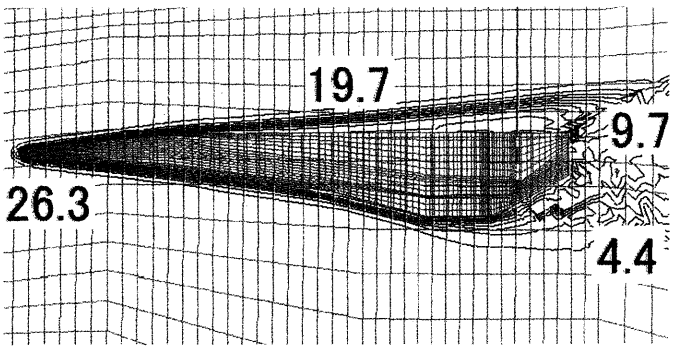

(c) Nondimensional temperature T/T_∞
(max T/T_∞=26.3)

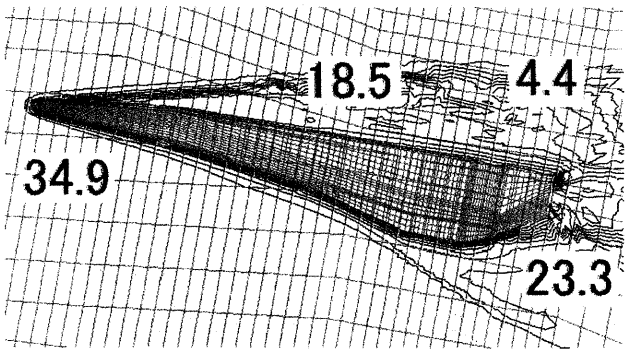

(c) Nondimensional temperature T/T_∞
(max T/T_∞=34.9)

Fig.10 Calculaed resuls of the flowfield.
(0-deg angle of attack)

Fig.11 Calculaed resuls of the flowfield.
(10-deg angle of attack)